Characterization of the Structure and Dynamics of the HDV Ribozyme at Different Stages Along the Reaction Path

Tai-Sung Lee,[†] George Giambaşu,[†] Michael E. Harris,[¶] and Darrin M. York[*,†]

BioMaPS Institute, Rutgers University, Piscataway, NJ 08854, USA, Department of Chemistry and Biological Chemistry, Rutgers University, Piscataway, NJ 08854, USA, and RNA Center and Department of Biochemistry, Case Western Reserve University School of Medicine, Cleveland, OH 44118, USA

E-mail: york@biomaps.rutgers,edu

[*]To whom correspondence should be addressed

[†]BioMaPS Institute, Rutgers University, Piscataway, NJ 08854, USA

[‡]Department of Chemistry and Biological Chemistry, Rutgers University, Piscataway, NJ 08854, USA

[¶]RNA Center and Department of Biochemistry, Case Western Reserve University School of Medicine, Cleveland, OH 44118, USA

The simulation setup is briefly summarized as follows:

The initial structure used in the reactant simulations (RT-C75^0-Mg) were based on a 2.45 Å crystal structure with two resolved Sr^{2+} ions (PDB: 1VC7).[1] The Sr^{2+} ions were replaced by native Mg^{2+} ions in the simulations. The C75U mutation was restored back to C75. The A-2 residue was removed and the position of the active site metal ion at the active site was changed to the position suggested by Chen et al.,[2] in which the active site Mg^{2+} directly binds to G1:N_7. Each simulation was performed in a cubic cell of $60\times60\times120$ Å^3 filled with pre-equilibrated TIP3P waters[3] with HDVr located at the center. The ion atmosphere consisted of Na^+ and Cl^- ions that were added to neutralize the system and reach the physiologic (extracellular) concentration of 0.14 M. The resulting system (the reactant state) contained 54,818 atoms: 16,914 water molecules, 2 Mg^{2+}, 102 Na^+, 43 Cl^-, 1,582 protein atoms, and 2,347 RNA atoms.

Simulations were performed with the NAMD simulation package (version 2.7b3)[4] using the AMBER[5,6] parm99 force field with the α/γ corrections for nucleic acids.[7]

Periodic boundary conditions were used along with the isothermal-isobaric ensemble (NPT) at 1 atm and 298 K using extended system pressure algorithm[8] with effective mass of 500.0 *amu* and Nosé-Hoover thermostat[9,10] with effective mass of 1000.0 kcal/mol-ps^2, respectively. The smooth particle mesh Ewald (PME) method[11,12] was employed with a B-spline interpolation order of 6, the default κ value (0.258 Å^{-1}), and 60, 60, and 120 FFT grid points were used for the x, y, and z cubic lattice directions, respectively. Non-bonded interactions were treated using an atom-based cutoff of 12 Å with switching of the non-bonded potential beginning at 10 Å. Numerical integration was performed using the leap-frog Verlet algorithm with 1 fs time step.[13] Covalent bond lengths involving hydrogen were constrained using the SHAKE algorithm.[14] For each simulation, 10 ns of water/ion equilibration followed by additional 10 ns of solute equilibration were performed before 350 ns of production simulation.

The initial structure of both the early (ETS) and late (LTS) transition state mimic were taken from the snapshot at 59.3 ns of the simulation of the deprotonated active reactant state. The initial structure of the product (Prod) simulation was taken from the snapshot at 130.0 ns of the simulation

of the late transition state mimic. The residue U-1 was removed with additional 5 ns ion/water equilibration performed prior to production simulation.

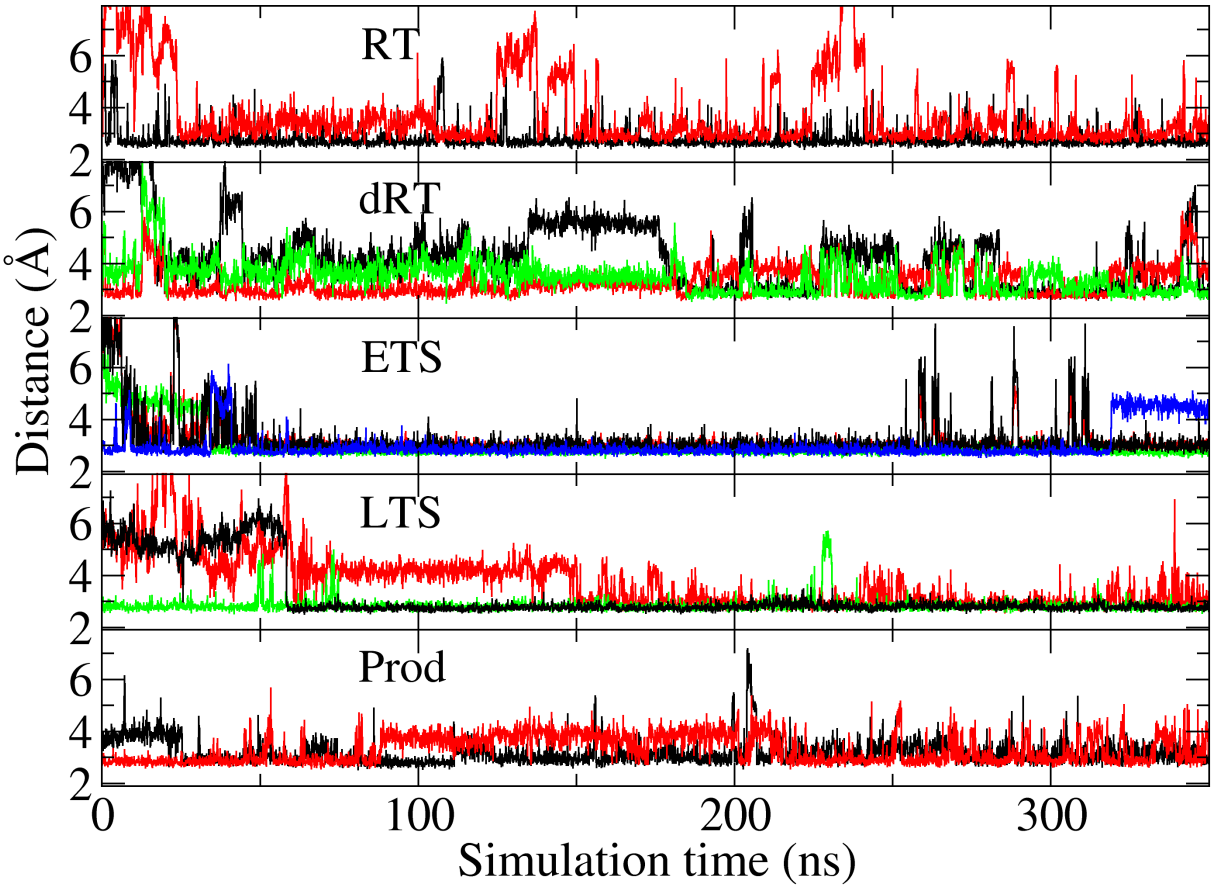

Figure 1: The time series of key H-Bond distances mentioned in the main text for different simulations: for RT: Black: G2:O_{2P} to U-1:$O_{2'}$; Red: C75:N_4 to G1:O_{2P} ; for dRT: Black: A77:N_6 to U-1:$O_{2'}$; Red: C75:N_3 to G1:O_{2P}; Green: C75:N_4 to G1:O_{2P} ; for ETS: Black: A78:N_6 to U-1:O_4; Red: A78:N_1 to U-1:N_3; Green: C75:N_4 to G1:O5'; Blue: C75:N_4 to C22:O_{2P}; for LTS: Black: C75:N_4 to G1:$O_{5'}$; Red: A77:N_6 to G1:O_{2P}; Green: C75:N_4 to C22:O_{2P}; for Prod: Black: C75:N_3 to G1:$O_{5'}$; Red: C75:N_4 to C22:O_{2P} .

References

(1) Ke, A.; Zhou, K.; Ding, F.; Cate, J. H. D.; Doudna, J. A. *Nature* **2004**, *429*, 201–205.

(2) Chen, J.-H.; Gong, B.; Bevilacqua, P. C.; Carey, P. R.; Golden, B. L. *Biochemistry* **2009**, *48*, 1498–1507.

(3) Jorgensen, W. L.; Chandrasekhar, J.; Madura, J. D.; Impey, R. W.; Klein, M. L. *J. Chem. Phys.* **1983**, *79*, 926–935.

(4) Phillips, J. C.; Braun, R.; Wang, W.; Gumbart, J.; Tajkhorshid, E.; Villa, E.; Chipot, C.; Skeel, R. D.; Kaleé, L.; Schulten, K. *J. Comput. Chem.* **2005**, *26*, 1781–1802.

(5) Case, D. A. et al. *AMBER 7*; University of California San Francisco: San Francisco, 2002.

(6) Pearlman, D. A.; Case, D. A.; Caldwell, J. W.; Ross, W. R.; Cheatham, III, T.; DeBolt, S.; Ferguson, D.; Seibel, G.; Kollman, P. *Comput. Phys. Commun.* **1995**, *91*, 1–41.

(7) Alberto Pérez,; Iván Marchán,; Svozil, D.; Sponer, J.; III, T. E. C.; Laughton, C. A.; Orozco, M. *Biophys. J.* **2007**, *92*, 3817–3829.

(8) Andersen, H. C. *J. Chem. Phys.* **1980**, *72*, 2384–2393.

(9) Nosé, S.; Klein, M. L. *Mol. Phys.* **1983**, *50*, 1055–1076.

(10) Hoover, W. G. *Phys. Rev. A* **1985**, *31*, 1695–1697.

(11) Essmann, U.; Perera, L.; Berkowitz, M. L.; Darden, T.; Hsing, L.; Pedersen, L. G. *J. Chem. Phys.* **1995**, *103*, 8577–8593.

(12) Sagui, C.; Darden, T. A. *Annu. Rev. Biophys. Biomol. Struct.* **1999**, *28*, 155–179.

(13) Allen, M.; Tildesley, D. *Computer Simulation of Liquids*; Oxford University Press: Oxford, 1987.

(14) Ryckaert, J. P.; Ciccotti, G.; Berendsen, H. J. C. *J. Comput. Phys.* **1977**, *23*, 327–341.